



Published in final edited form as:

Science. 2019 August 09; 365(6453): 559–565. doi:10.1126/science.aay0198.

A vicious cycle of amyloid β -dependent neuronal hyperactivation

Benedikt Zott^{1,2}, Manuel M. Simon^{1,2}, Wei Hong³, Felix Unger^{1,2}, Hsing-Jung Chen-Engerer^{1,2}, Matthew P. Frosch⁴, Bert Sakmann¹, Dominic M. Walsh³, Arthur Konnerth^{1,2,*}

¹Institute of Neuroscience, Technical University of Munich, 80802 Munich, Germany

²Munich Cluster for Systems Neurology, Technical University of Munich, 80802 Munich, Germany

³Laboratory for Neurodegenerative Research, Ann Romney Center for Neurologic Diseases, Brigham and Women's Hospital, and Harvard Medical School, Boston, Massachusetts 02115, USA

⁴C.S. Kubik Laboratory for Neuropathology, Massachusetts General Hospital, Boston, Massachusetts, USA

Abstract

Amyloid β ($A\beta$)-dependent neuronal hyperactivity is believed to contribute to the circuit dysfunction which characterizes the early stages of Alzheimer's disease (AD). While experimental evidence in support of this hypothesis continues to accrue, the underlying pathological mechanisms are not well understood. Here we used mouse models of $A\beta$ -amyloidosis, to show that hyperactivation is initiated by the suppression of glutamate reuptake. Hyperactivity occurred in neurons with pre-existing baseline activity, whereas inactive neurons were generally resistant to $A\beta$ -mediated hyperactivation. $A\beta$ -containing AD brain extracts and purified $A\beta$ dimers were able to sustain this vicious cycle. Our findings suggest a cellular mechanism of $A\beta$ -dependent neuronal dysfunction that can be active prior to plaque formation.

One Sentence Summary:

Mechanism of $A\beta$ -dependent neuronal hyperactivity.

Main Text:

The progressive buildup of $A\beta$ in the brains of AD patients is a firmly established experimental observation (1,2). The consequences of this buildup are manifold and include synaptic dysfunction, inflammation and, ultimately, cell death (3,4). On the systems level, functional brain changes such as impaired neuronal activity and disturbed brain metabolism

*Correspondence to: arthur.konnerth@tum.de.

Author contributions: BZ and AK conceived the study. All authors planned experiments. BZ, MMS, WH, FU and HC performed the experiments. All authors interpreted the data. BZ and AK wrote the first draft of the manuscript. All authors read and commented on the manuscript.

Competing interests: None of the authors have biomedical financial interests or potential conflicts of interest related to the work performed in the present study. Unrelated to the current study, D.M.W. is an advisor to CogRx and Regeneron, and has active collaborations with Medimmune, Sanofi, Gen2 and Roche. D.M.W. joined Biogen.

Data and materials availability: All data is available in the main text or the supplementary materials.

have been associated with A β -amyloidosis (5–7). Several lines of evidence indicate that neuronal hyperactivity is a potential key feature of early stages of AD. Both in mice and man there is strong evidence of excessive neuronal activation that under certain conditions can induce epileptic seizures (8–10). Functional imaging studies in individuals with prodromal AD reveals increased neuronal activity in the hippocampus and some neocortical areas (6). The cellular correlates of this hyperactivity have been studied in mouse models of A β -amyloidosis using two-photon calcium imaging (11,12) and implicate an essential role for soluble A β (11).

An open question for understanding AD pathology is how soluble A β mediates cellular dysfunction such as hyperactivity. A large number of possible A β “receptors” have been suggested (13) but their roles in neuronal dysfunction in vivo has not been elucidated. Ample evidence points towards an A β -dependent impairment at both inhibitory (5, 8, 10) and excitatory (14–17) synapses. Specifically, an impairment of glutamate homeostasis is evident in rodents (18–21) and humans (22,23) and might underlie the disturbed plasticity of hippocampal synapses (18, 19). However, the link between impaired glutamate homeostasis and neuronal function in vivo is unclear. Here, we explored the mechanism of A β -dependent neuronal hyperactivation and the forms of soluble A β which mediate this cellular dysfunction.

Neuronal hyperactivity requires pre-existing baseline activity

We used two-photon Ca²⁺ imaging of hippocampal CA1 neurons in vivo (11) (Fig. S1, A–C) to test the direct action of soluble A β . Synthetic A β (1–40)S26C, in which the naturally occurring serine at position 26 was replaced with cysteine, was used to produce and test the effects of the disulphide cross-linked dimer [A β S26C]₂ (24, 25). [A β S26C]₂ was pressure applied near the CA1 hippocampal pyramidal layer of 1–2 month-old wild-type (WT) mice. In most neurons application of 500 nM [A β S26C]₂ induced reversibly a massive increase in activity similar to the hyperactivity seen in APP transgenic mice (11) (Fig. 1A, control experiments in fig. S1D and E). Intriguingly, applications of [A β S26C]₂ were ineffective in hippocampal slices (Fig. 1B, fig. S2, A and B). A possible explanation for these apparently contradictory findings was that the neuronal ‘baseline’ activity was greatly reduced in hippocampal slices compared to in vivo (fig. S2, C and D). Here, to test the role of baseline activity for A β -induced neuronal hyperactivation we performed ‘loss’-of-(dys)function experiments in the hippocampus of WT mice in vivo and ‘gain’-of-(dys)function in hippocampal slices. First, we demonstrated that application of [A β S26C]₂ was ineffective when blocking in vivo neuronal activity by antagonists ionotropic glutamate receptors (Fig. 1C, E) or by the sodium channel antagonist tetrodotoxin (TTX) (Fig. S3). Next, we turned to the analysis of hippocampal slices in vitro and did opposite experiments in which we induced in vivo-like baseline activity through various pharmacological manipulations. Treatments included: (1) block of GABAergic synaptic inhibition by bicuculline, (2) addition of glutamate to the bath, (3) elevation of the extracellular K⁺ concentration, and (4) combinations of these manipulations. Each of these treatments induced an average baseline activity that was similar to that detected under in vivo conditions (fig. S4A). Baseline activity increased in the presence of bicuculline in 5 representative neurons as illustrated in Fig. 1D, left. In these conditions, the application of [A β S26C]₂ resulted in a reversible

increase of additional activity (Fig. 1D, F). A similar effect was observed by the addition of low levels of glutamate (Fig. 1G) or by the elevation of the extracellular potassium concentration (Fig. 1H, for controls see fig. S4B–D). In studies on the A β -dependence of activity-dependent synaptic plasticity, such as long-term potentiation (LTP) (e.g. (19, 24)) or long-term depression (LTD) (e.g. (18, 26)), an increase of baseline activity is probably not necessary, because the induction protocols for synaptic plasticity involve increased levels of activity. In conclusion, our *in vitro* experiments support the *in vivo* observations and indicate that increased levels of baseline activity are a pre-requisite for [A β S26C]₂-induced hyperactivity. Cell-by-cell analyses show that, despite a considerable variance, there is on average a positive correlation between baseline activity and the degree of hyperactivation (Fig. 1I, fig. S4E).

Hyperactivation through an A β -dependent block of glutamate reuptake

Under *in vivo* conditions neuronal activity generated by glutamatergic excitation was required for [A β S26C]₂-induced hyperactivity (Fig. 1C). In our search for a cause underlying a synaptic potentiation we considered pre- and postsynaptic mechanisms. To investigate if [A β S26C]₂ acted pre-synaptically, we performed paired-pulse facilitation experiments and tested for possible changes of presynaptic release probability of glutamate (27). Application of [A β S26C]₂ had no detectable impact on paired-pulse facilitation (fig. S5), as expected (18, 24, 28). An alternative hypothesis was inspired by reports on an A β -dependent defect of the glutamate homeostasis, possibly involving an impairment of glutamate reuptake (18–20). In a first step, we tested whether pharmacologically blocking glutamate uptake *in vivo* had any detectable effect on neuronal activity. For this, we used the unspecific glutamate uptake blocker DL-threo- β -benzyloxyaspartic acid (TBOA), which can mimic some effects of A β on activity-dependent synaptic plasticity *in vitro* (18, 19). The local application of TBOA to hippocampal CA1 neurons in WT mice induced neuronal hyperactivity (Fig. 2A and B), an effect that was similar to that observed with [A β S26C]₂ applications (Fig. 1A and E, Fig. 2C). Nevertheless, [A β S26C]₂ and TBOA may have exerted their actions through different mechanisms. To address this issue, we repeated the experiments in the transgenic APP23 x PS45 mouse model of A β -amyloidosis (12). We used young mice with no obvious amyloid plaques, but high levels of soluble A β (12) and a pronounced hippocampal hyperactivity (11) (Fig. 2D and E; fig. S6). Application of TBOA had a strong hyperactivating action in WT mice (Fig. 2F) but almost no effect in APP23 x PS45 mice (Fig. 2G and I). Applications of [A β S26C]₂ were also ineffective in APP23 x PS45 mice (Fig. 2, H and J). Thus, endogenous A β largely occluded both TBOA or [A β S26C]₂-induced hyperactivation.

Strong enhancement of synaptic stimulation-evoked glutamate transients through A β

To further test this glutamate accumulation hypothesis, we used two-photon glutamate imaging involving the viral expression of the fluorescent glutamate sensor iGluSnFr (29). For this purpose, an iGluSnFr viral construct was injected unilaterally into the hippocampal CA1 region *in vivo* (Fig. 3A), leading after three weeks to a strong and dense neuronal

expression of iGluSnFr (Fig. 3B). In parallel, we also performed as controls sparse labelling experiments of CA1 pyramidal neurons (Fig. 3C). In order to induce synaptic glutamate release, we electrically stimulated a bundle of afferent Schaffer collateral axons in hippocampal slices. We performed two-photon glutamate imaging and collected the bulk response in a region of interest (Fig. 3D, **inset**), which covered a substantial part of the glutamate sensor-expressing dendrites of CA1 neurons (Fig. 3C). Single-shock stimulation produced large transient increases in extracellular glutamate concentration (Fig. S7A, control experiments in fig. S7B and C). Local application of A β produced a strong and reversible potentiation of the glutamate transients (Fig 3D and E, fig. S7D). Similar glutamate transients were induced by applications of TBOA (Fig 3F and G, fig. S7D). Thus, peri-synaptic glutamate accumulations, through impaired uptake of synaptically-released glutamate, may drive A β -dependent hyperactivity. In line with this conclusion, whole-cell recordings of NMDA receptor-dependent excitatory postsynaptic currents (NMDA-epscs) in CA1 pyramidal cells of hippocampal slices (30) were similarly affected by both TBOA and [A β S26C]₂ (fig. S8). Together, these results demonstrate that TBOA and [A β S26C]₂ act through a similar, yet unknown, molecular mechanism.

The astro-glial excitatory amino-acid transporter (EAAT)-2 (also termed GLT-1 in mice) is the predominant EAAT in the hippocampal CA1 region. Therefore, we tested whether A β interferes with EAAT2-mediated glutamate uptake. First, we tested the GLT-1 antagonist Dihydrokainic acid (DHK) in WT mice. Similar to TBOA and [A β S26C]₂, DHK caused robust neuronal hyperactivity (fig. S9A and B). Furthermore, the cross-linking GLT-1 antibody (GLT-1 AB) also induced hyperactivity (Fig. 3H and I, for controls see fig. S9C and D). Cross-linking GLT-1 ABs can impair glutamate uptake by obstructing lateral membrane diffusion of glutamate/GLT-1 complexes along astrocytic protrusions out of the synaptic cleft - a process suggested to be essential for clearing synaptically released glutamate (31). Our results using DHK, GLT1 and A β suggest that the A β -dependent block of glutamate reuptake may not involve A β binding to transporter proteins, but rather perturbation of astrocytic membrane dynamics and obstruction of GLT-1 diffusion (31).

Effectiveness of human A β species derived from Alzheimer's patients

To further explore the relevance of our findings to the human disease, we employed forms of A β derived from AD brain. First, we used A β -containing AD brain extracts (32). When examined by immunoprecipitation/immunoblotting, the A β in such brain extracts migrate on denaturing SDS-PAGE with molecular weights indicative of monomers and SDS-stable dimers. A β -containing AD extracts (Fig. 4A), but not those immunodepleted of A β (ID extract, Fig. 4B) are capable of inducing a variety of disease-relevant effects (24, 33–35). In vivo local applications of AD extract to CA1 neurons of WT mice produced a marked neuronal hyperactivity (Fig. 4C, D and F), whereas the ID extract did not induce hyperactivity (fig. S10, A and B). Similarly, when tested in vitro, AD extract induced hyperactivity in active hippocampal CA1 neurons treated with bicuculline (Fig. 4E and G), but ID extract had no effect (fig. S10C and D). Moreover, AD extract failed to cause hyperactivation in vivo in the presence of D-APV and CNQX (fig. S10E and F), or in unmanipulated hippocampal slices (fig. S10G and H).

Purified AD brain-derived cross-linked dimers can block long-term potentiation (LTP) and impair neuritic integrity (36). We thus investigated if such material (fig. S11A) could also induce hyperactivity. As a control, we isolated A β monomer from the same AD brain (fig. S11A). A β dimers, but not equimolar A β monomers (36, 37) (fig. S11, B–E) reduced neurite length (fig. S11, B and C) and the number of branch points (fig. S11, D and E). Similarly, the application of brain-derived A β dimers effectively, but reversibly, induced hyperactivity WT mice in vivo (Fig. 5A and B). Noteworthy, human A β dimers induced similar levels of hyperactivity at substantially lower concentrations than the synthetic ones (0.2 μ g/ml human vs. 4.3 μ g/ml synthetic A β dimers). The application of human A β monomers had little or no effect (Fig. 5E). The activity of dimers was highly dose-dependent, with an apparent EC₅₀ of 27.5 ng/ml (Fig. 5C). Application of AD brain-derived A β dimers to bicuculline-treated mouse hippocampal slices reliably induced hyperactivity in neurons with a high baseline activity (fig. S12) and produced an activity-dependent hyperactivation in vivo (Fig 5D). Finally, when A β monomers were applied to hippocampal CA1 neurons they had little or no ability to induce hyperactivation both in vivo and in vitro (Fig S13).

Discussion and conclusions

In this study, we characterized rapid actions of synthetic and AD brain-derived A β on the activity of mouse hippocampal neurons in vitro and in vivo. Our findings suggest that A β can induce hyperexcitation in sensitive neurons and that this drives a vicious cycle of hyperactivation (Fig. 5F). To explain the scheme, we start out with the insight that there is a simple solution to the puzzle that A β -dependent hyperactivity is readily observed in vivo, but not in vitro. We were able to show that there is an absolute need of ongoing activity for the induction of A β -dependent synaptic hyperactivation. Next, the block of synaptically-released glutamate at active excitatory synapses is an important element of the vicious cycle. The third component of the cycle is excessive peri-synaptic accumulation of glutamate. The final element of the cycle is revealed by the dependence of the increase in hyperactivation on the level of baseline activity, both for synthetic and human brain-derived A β dimers. It is important to note that this process of amplification appears to be self-limited at high levels of hyperactivity, as indicated by the results of the occlusion experiments. Thus, multiple lines of evidence underscore the role of all four elements of the cycle.

While the dependence of hyperactivation on impaired excitatory synaptic transmission involving defective glutamate reuptake had not previously been predicted, there is prior evidence for impaired glutamate homeostasis both in rodents (18–21) and AD patients (22,23). Furthermore, there is evidence for beneficial effects of certain anti-glutamatergic drugs, such as memantine, against AD (20, 38–40). It is suggested that these drugs may act peri-synaptically on extrasynaptic NMDA receptors (40). Moreover, this process may be aggravated by pathologically-reduced expression levels of glutamate transporters, such as EAAT2 in AD patients (22) or by reduced levels of synaptic inhibition (5, 8, 10). Finally, it is important to stress that A β -dependent hyperactivity precedes plaque formation and that it is present at early stages, long before overt clinical symptoms of AD (6). A gradual neuronal “silencing” occurs after plaques are formed and may be the prelude to neurodegeneration (41). While functional deficits of circuits caused by massive degeneration are nearly impossible to be repaired with current approaches, it may be possible to therapeutically

target hyperactivation at early stages of the disease by lowering A β levels, reducing neuronal activity by enhancing synaptic inhibition, or by pharmacological manipulations of EAATs.

Supplementary Material

Refer to Web version on PubMed Central for supplementary material.

Acknowledgments:

We thank Christine Karrer, Christian Obermayer, Felix Beyer and Rosa Maria Karl for technical support. We are grateful to Dr. Loren Looger for providing iGlu-SnFr constructs.

Funding: This work was supported by the Deutsche Forschungsgemeinschaft (SFB 870) and a European Research Council Advanced Grant to AK, and by grants to DMW from the National Institutes of Health (AG046275), Bright Focus, and by the Massachusetts Alzheimer's Disease Research Center (AG05134). DMW is an Alzheimer Association Zenith Fellow. AK is a Hertie-Senior-Professor for Neuroscience.

References and Notes:

1. Selkoe DJ, Hardy J, The amyloid hypothesis of Alzheimer's disease at 25 years. *EMBO molecular medicine* 8, 595–608 (2016). [PubMed: 27025652]
2. Musiek ES, Holtzman DM, Three dimensions of the amyloid hypothesis: time, space and “wingmen”. *Nature Neuroscience* 18, 800 (2015). [PubMed: 26007213]
3. De Strooper B, Karran E, The Cellular Phase of Alzheimer's Disease. *Cell* 164, 603–615 (2016). [PubMed: 26871627]
4. Viola KL, Klein WL, Amyloid β oligomers in Alzheimer's disease pathogenesis, treatment, and diagnosis. *Acta Neuropathologica* 129, 183–206 (2015). [PubMed: 25604547]
5. Palop JJ, Mucke L, Network abnormalities and interneuron dysfunction in Alzheimer disease. *Nat Rev Neurosci* 17, 777–792 (2016). [PubMed: 27829687]
6. Zott B, Busche MA, Sperling RA, Konnerth A, What Happens with the Circuit in Alzheimer's Disease in Mice and Humans? *Annual Review of Neuroscience* 41, 277–297 (2018).
7. Wang Z et al., Human Brain-Derived A β Oligomers Bind to Synapses and Disrupt Synaptic Activity in a Manner That Requires APP. *The Journal of neuroscience : the official journal of the Society for Neuroscience* 37, 11947–11966 (2017).
8. Verret L et al., Inhibitory interneuron deficit links altered network activity and cognitive dysfunction in Alzheimer model. *Cell* 149, 708–721 (2012). [PubMed: 22541439]
9. Vossel KA et al., Seizures and epileptiform activity in the early stages of Alzheimer disease. *JAMA neurology* 70, 1158–1166 (2013). [PubMed: 23835471]
10. Palop JJ et al., Aberrant excitatory neuronal activity and compensatory remodeling of inhibitory hippocampal circuits in mouse models of Alzheimer's disease. *Neuron* 55, 697–711 (2007). [PubMed: 17785178]
11. Busche MA et al., Critical role of soluble amyloid-beta for early hippocampal hyperactivity in a mouse model of Alzheimer's disease. *Proc Natl Acad Sci U S A* 109, 8740–8745 (2012). [PubMed: 22592800]
12. Busche MA et al., Clusters of hyperactive neurons near amyloid plaques in a mouse model of Alzheimer's disease. *Science* 321, 1686–1689 (2008). [PubMed: 18802001]
13. Jarosz-Griffiths HH, Noble E, Rushworth JV, Hooper NM, Amyloid- β Receptors: The Good, the Bad, and the Prion Protein. *Journal of Biological Chemistry* 291, 3174–3183 (2016). [PubMed: 26719327]
14. Shankar GM et al., Natural oligomers of the Alzheimer amyloid-beta protein induce reversible synapse loss by modulating an NMDA-type glutamate receptor-dependent signaling pathway. *J Neurosci* 27, 2866–2875 (2007). [PubMed: 17360908]

15. Koffie RM et al., Oligomeric amyloid beta associates with postsynaptic densities and correlates with excitatory synapse loss near senile plaques. *Proc Natl Acad Sci U S A* 106, 4012–4017 (2009). [PubMed: 19228947]
16. Um Ji W. et al., Metabotropic Glutamate Receptor 5 is a Coreceptor for Alzheimer A β Oligomer Bound to Cellular Prion Protein. *Neuron* 79, 887–902 (2013). [PubMed: 24012003]
17. Lerdkrai C et al., Intracellular Ca²⁺ stores control in vivo neuronal hyperactivity in a mouse model of Alzheimer's disease. *Proc Natl Acad Sci U S A* 115, 1279–1288 (2018).
18. Li S et al., Soluble oligomers of amyloid Beta protein facilitate hippocampal long-term depression by disrupting neuronal glutamate uptake. *Neuron* 62, 788–801 (2009). [PubMed: 19555648]
19. Li S et al., Soluble A β oligomers inhibit long-term potentiation through a mechanism involving excessive activation of extrasynaptic NR2B-containing NMDA receptors. *The Journal of neuroscience* 31, 6627–6638 (2011). [PubMed: 21543591]
20. Hefendehl JK et al., Mapping synaptic glutamate transporter dysfunction in vivo to regions surrounding A β plaques by iGluSnFR two-photon imaging. *Nature Communications* 7, 13441 (2016).
21. O'Shea SD et al., Intracerebroventricular Administration of Amyloid β -protein Oligomers Selectively Increases Dorsal Hippocampal Dialysate Glutamate Levels in the Awake Rat. *Sensors (Basel, Switzerland)* 8, 7428–7437 (2008).
22. Masliah E, Hansen L, Alford M, Deteresa R, Mallory M, Deficient glutamate transport is associated with neurodegeneration in Alzheimer's disease. *Annals of Neurology* 40, 759–766 (1996). [PubMed: 8957017]
23. Scott HA, Gebhardt FM, Mitrovic AD, Vandenberg RJ, Dodd PR, Glutamate transporter variants reduce glutamate uptake in Alzheimer's disease. *Neurobiology of Aging* 32, 553.e551–553.e511 (2011).
24. Shankar GM et al., Amyloid-beta protein dimers isolated directly from Alzheimer's brains impair synaptic plasticity and memory. *Nat Med* 14, 837–842 (2008). [PubMed: 18568035]
25. O'Nuallain B et al., Amyloid β -Protein Dimers Rapidly Form Stable Synaptotoxic Protofibrils. *The Journal of Neuroscience* 30, 14411–14419 (2010). [PubMed: 20980598]
26. Hsieh H et al., AMPAR removal underlies A β -induced synaptic depression and dendritic spine loss. *Neuron* 52, 831–843 (2006). [PubMed: 17145504]
27. Manabe T, Wyllie DJ, Perkel DJ, Nicoll RA, Modulation of synaptic transmission and long-term potentiation: effects on paired pulse facilitation and EPSC variance in the CA1 region of the hippocampus. *Journal of Neurophysiology* 70, 1451–1459 (1993). [PubMed: 7904300]
28. Zhao J et al., Soluble A β Oligomers Impair Dipolar Heterodendritic Plasticity by Activation of mGluR in the Hippocampal CA1 Region. *iScience* 6, 138–150 (2018). [PubMed: 30240608]
29. Marvin JS et al., Stability, affinity, and chromatic variants of the glutamate sensor iGluSnFR. *Nature Methods* 15, 936–939 (2018). [PubMed: 30377363]
30. Arnth-Jensen N, Jabaudon D, Scanziani M, Cooperation between independent hippocampal synapses is controlled by glutamate uptake. *Nature Neuroscience* 5, 325 (2002). [PubMed: 11896395]
31. Murphy-Royal C et al., Surface diffusion of astrocytic glutamate transporters shapes synaptic transmission. *Nature Neuroscience* 18, 219 (2015). [PubMed: 25581361]
32. Hong W et al., Diffusible, highly bioactive oligomers represent a critical minority of soluble A β in Alzheimer's disease brain. *Acta Neuropathologica* 136, 19–40 (2018). [PubMed: 29687257]
33. Borlikova GG et al., Alzheimer brain-derived amyloid β -protein impairs synaptic remodeling and memory consolidation. *Neurobiology of aging* 34, 1315–1327 (2013). [PubMed: 23182244]
34. Mc Donald JM et al., The aqueous phase of Alzheimer's disease brain contains assemblies built from ~4 and ~7 kDa A β species. *Alzheimer's & dementia : the journal of the Alzheimer's Association* 11, 1286–1305 (2015).
35. Freir DB et al., Interaction between prion protein and toxic amyloid β assemblies can be therapeutically targeted at multiple sites. *Nature communications* 2, 336 (2011).
36. Brinkmalm G et al., Identification of neurotoxic cross-linked A β dimers in Alzheimer brain. *Brain* (2019).

37. Jin M et al., An in vitro paradigm to assess potential anti-A β antibodies for Alzheimer's disease. *Nature Communications* 9, 2676 (2018).
38. Takahashi K et al., Restored glial glutamate transporter EAAT2 function as a potential therapeutic approach for Alzheimer's disease. *The Journal of experimental medicine* 212, 319–332 (2015). [PubMed: 25711212]
39. Zumkehr J et al., Ceftriaxone ameliorates tau pathology and cognitive decline via restoration of glial glutamate transporter in a mouse model of Alzheimer's disease. *Neurobiology of aging* 36, 2260–2271 (2015). [PubMed: 25964214]
40. Danysz W, Parsons CG, Möbius H-J, Stöffler A, Quack G, Neuroprotective and symptomatological action of memantine relevant for alzheimer's disease — a unified glutamatergic hypothesis on the mechanism of action. *Neurotoxicity Research* 2, 85–97 (2000). [PubMed: 16787834]
41. Busche MA, Konnerth A, Neuronal hyperactivity--A key defect in Alzheimer's disease? *Bioessays* 37, 624–632 (2015). [PubMed: 25773221]
42. Franklin K, Paxinos G, The mouse brain in stereotaxic coordinates, compact. The coronal plates and diagrams.
43. Busche MA et al., Decreased amyloid-beta and increased neuronal hyperactivity by immunotherapy in Alzheimer's models. *Nat Neurosci* 18, 1725–1727 (2015). [PubMed: 26551546]
44. Stosiek C, Garaschuk O, Holthoff K, Konnerth A, In vivo two-photon calcium imaging of neuronal networks. *Proceedings of the National Academy of Sciences* 100, 7319 (2003).
45. Tada M, Takeuchi A, Hashizume M, Kitamura K, Kano M, A highly sensitive fluorescent indicator dye for calcium imaging of neural activity in vitro and in vivo. *European Journal of Neuroscience* 39, 1720–1728 (2014). [PubMed: 24405482]
46. Keskin AD et al., BACE inhibition-dependent repair of Alzheimer's pathophysiology. *Proc Natl Acad Sci U S A* 114, 8631–8636 (2017). [PubMed: 28739891]
47. Ferreira JS et al., Co-agonists differentially tune GluN2B-NMDA receptor trafficking at hippocampal synapses. *eLife* 6, e25492 (2017). [PubMed: 28598327]
48. Stocca G, Vicini S, Increased contribution of NR2A subunit to synaptic NMDA receptors in developing rat cortical neurons. *The Journal of physiology* 507, 13–24 (1998). [PubMed: 9490809]
49. Benner S, Kakeyama M, Endo T, Yoshioka W, Tohyama C, Application of NeuroTrace staining in the fresh frozen brain samples to laser microdissection combined with quantitative RT-PCR analysis. *BMC Research Notes* 8, 252 (2015). [PubMed: 26092293]

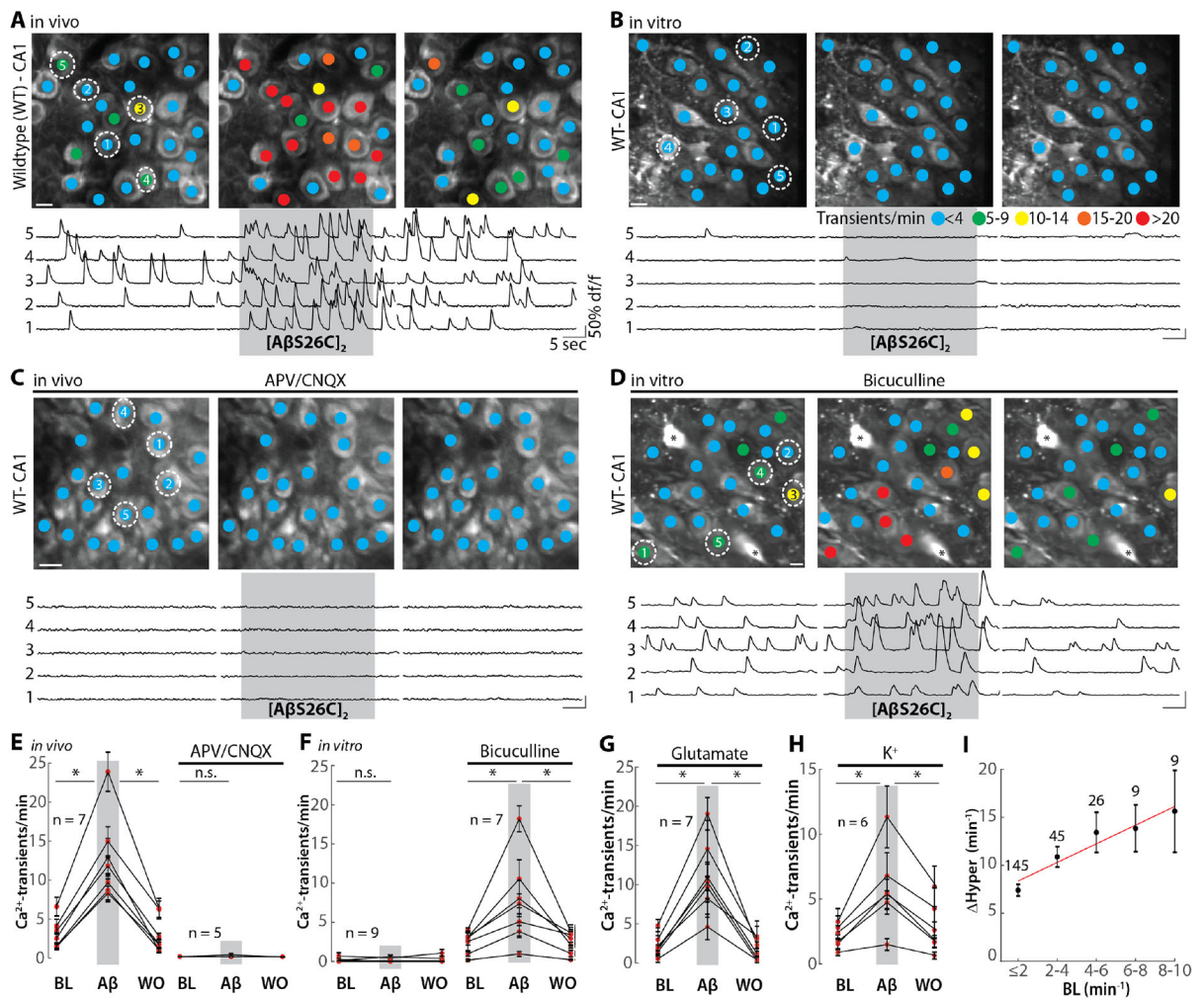


Fig. 1. Activity-dependence of the A β -dependent neuronal hyperactivation

(A) Top: representative two-photon images of the hippocampal CA1 region of a wild-type mouse *in vivo* before (left), during the application of 500 nM [A β S26C]₂ (middle) and after 5–10 min of washout (right). The colored dots on the neurons indicate the number of Ca²⁺-transients per minute. Bottom: Ca²⁺-traces of the five neurons circled in the top panel. The grey shaded area indicates the time period of [A β S26C]₂ application. (B) Top: representative two-photon images of the hippocampal CA1 region of an acute slice preparation before (left), during [A β S26C]₂ application (middle) and after washout (right). Bottom: Ca²⁺-traces of the five neurons circled in the top panel. The grey shaded area indicates the period of [A β S26C]₂ application. (C) Same as (A) for a mouse in which glutamatergic transmission was blocked by bath application of D-APV (50 μ M) and CNQX (50 μ M). (D) Same as (B) for a slice treated with 80 μ M bicuculline and an elevated potassium concentration (6.5 mM). The asterisks denote astrocytes. (E) Summary data of the *in vivo* experiments in (A) (left) and (C) (right). Each dot represents the mean under baseline (BL), [A β S26C]₂ application and washout (WO) conditions. (F). Same as (E) for experiments in (B) and (D). (G) Summary data of the *in vitro* experiments in which neuronal baseline activity was induced by the superfusion of glutamate (40–60 μ M). (H) Summary data of *in vitro*

experiments in which neuronal baseline activity was induced by elevating extracellular K^+ (to 7.5–8.5 mM). (I) Plot of baseline activity (BL) vs. $[A\beta S26C]_2$ -dependent relative increase in activity in vivo (DHyper) for individual neurons. The numbers for neurons for each bin of BL activity is indicated in the graph. Red line: linear fit. Scale bars: 5 μm . Error bars show SEM. Wilcoxon signed rank test, * $P < 0.05$; n.s. not significant.

Author Manuscript

Author Manuscript

Author Manuscript

Author Manuscript

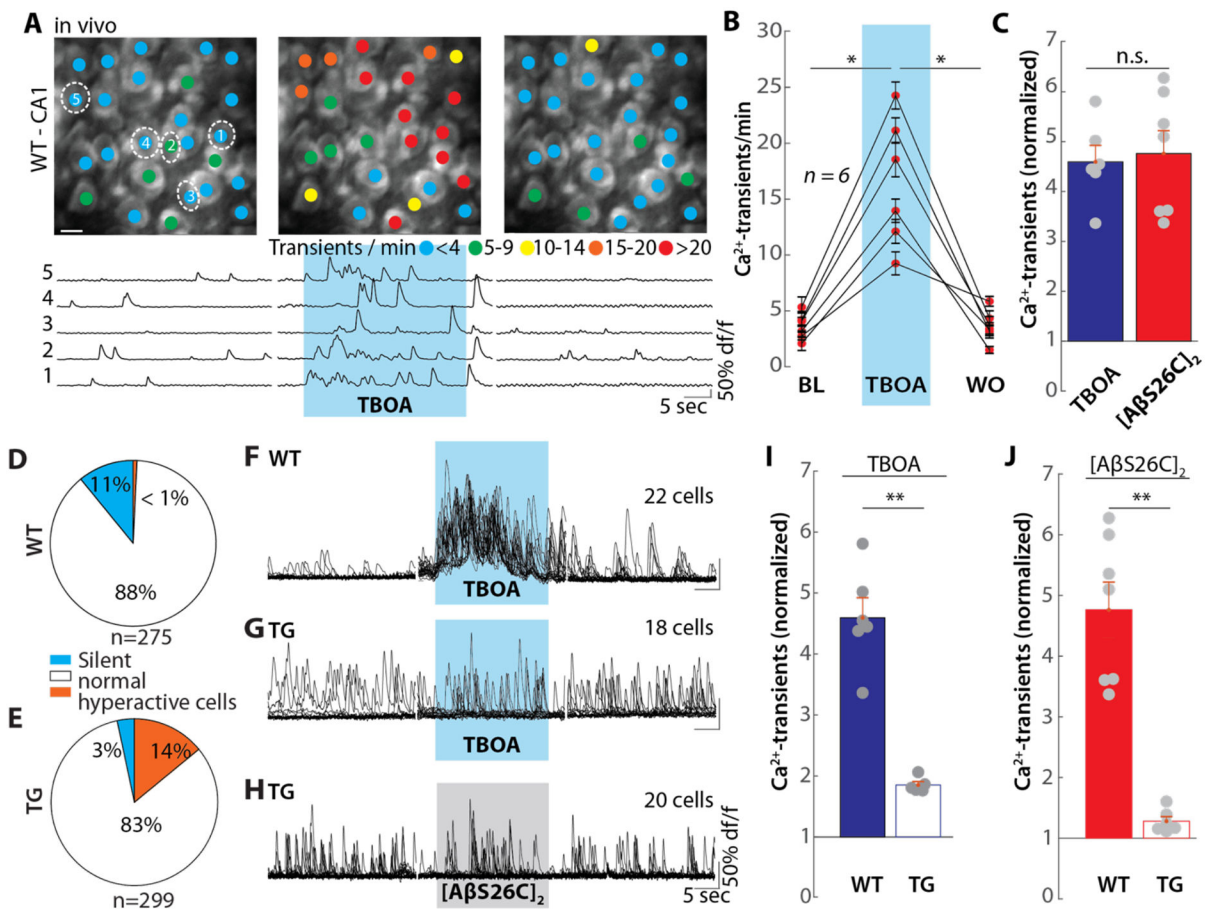


Fig. 2. [AβS26C]₂-dependent suppression of glutamate re-uptake.

(A) Same experimental arrangement as in Fig. 1A, but application of 250 μM DL-TBOA. (B) Summary data for the experiment in (A). Each dot represents the mean number of Ca^{2+} -transients per minute for all neurons in one mouse under baseline (BL), TBOA application and washout (WO) conditions. (C) Bar graph showing the normalized number of Ca^{2+} -transients. Each point represents the mean number of Ca^{2+} -transients in one mouse during application of 500 nM [AβS26C]₂ (left, n = 7 mice), or TBOA (right, n = 7), normalized to baseline. (D and E) pie chart depicting the proportion of silent (blue), normal (white) and hyperactive (orange) neurons in wildtype (D) (n = 275 cells from 7 mice) and APP23 x PS45 transgenic (TG) mice (E) (n = 299 cells from 6 mice). (F and G) Overlaid Ca^{2+} -traces from all neurons in one wild type mouse (F) and one APP23 x PS45 mouse (G) for baseline (left), TBOA application (middle) and washout (right) conditions. The blue shaded area corresponds to the time of TBOA application. (H) Overlaid Ca^{2+} -traces from all neurons (n = 20 cells) in one APP23 x PS45 mouse for baseline (left), [AβS26C]₂ application (middle) and washout (right) conditions. The grey shaded area indicates the period of [AβS26C]₂ application. (I) Bar graph of the normalized activity during the application of TBOA in wildtype (WT, left, solid bars, n = 7) or APP23 x PS45 transgenic (TG, right, open bars, n = 5) mice. Each point represents the mean number of Ca^{2+} -transients in one mouse during the application of TBOA, normalized to baseline. (J) Same as (I) for the application of

[A β S26C]₂ in WT (n = 6) or TG (n = 6) mice. Error bars show SEM. Wilcoxon signed rank test (D, E) or Wilcoxon rank sum test (F), **P<0.005, *P<0.05; n.s. not significant.

Author Manuscript

Author Manuscript

Author Manuscript

Author Manuscript

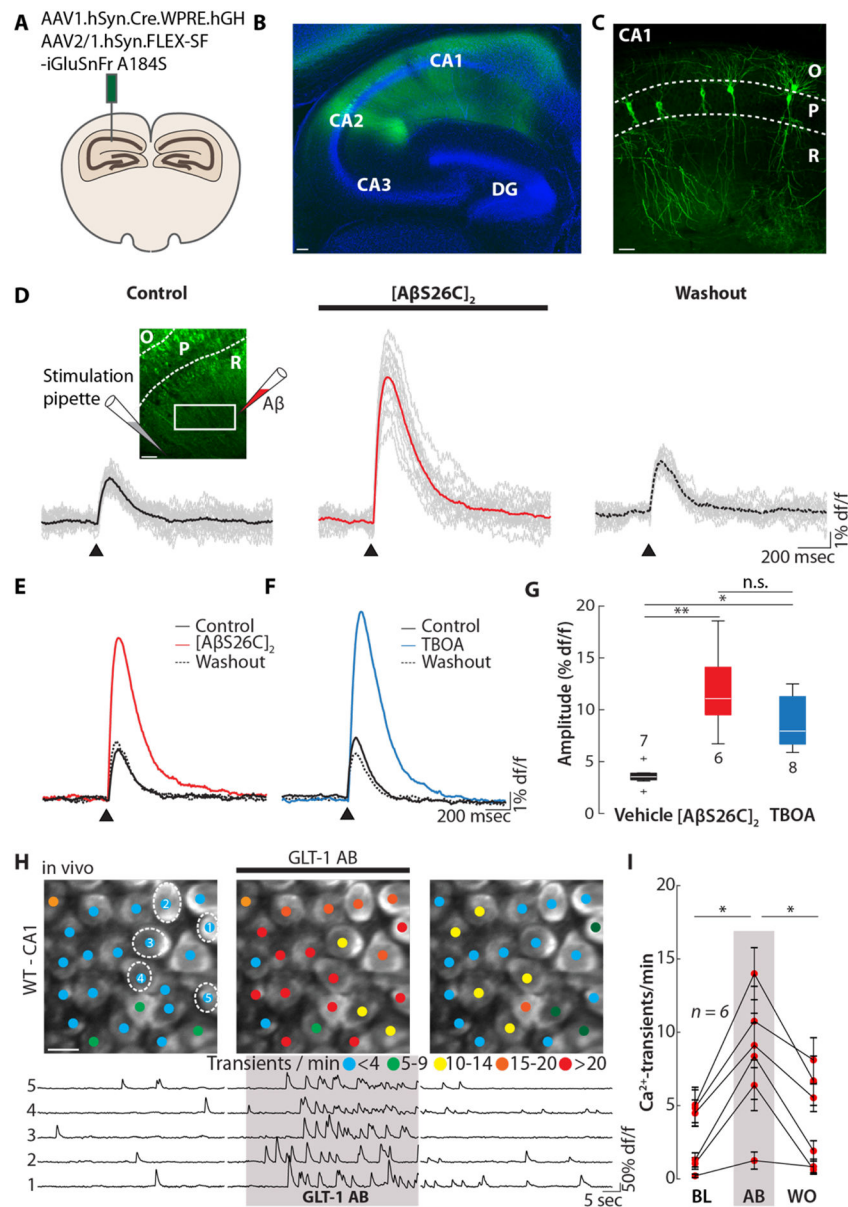


Fig. 3. [AβS26C]₂-dependent potentiation of synaptic stimulation-evoked glutamate transients. (A) Scheme of the injection of SF-iGluSnFr A184S into the mouse hippocampal CA1 region. (B) Confocal image of a hippocampal slice 21 days post-injection with SF-iGluSnFr (green). Cell bodies are stained with Neurotrace (blue). Scale bar: 100 μm. (C) Sparse labelling of the hippocampal CA1 neurons with SF-iGlu-SnFr. The dashed lines indicate the pyramidal layer (P) of the hippocampal CA1 region. O, stratum oriens; R, stratum radiale. Scale bar: 50 μm. (D) Individual (grey) mean (color) glutamate transients collected in a rectangular region of interest in the stratum radiatum (inset left) after electrical stimulation (arrow head, 100 μs/40V) before (left), during the application of 500 nM [AβS26C]₂ (middle) and after washout (right). The inset indicates the positions of the stimulation and the [AβS26C]₂-application pipettes, respectively. Scale bar: 50 μm. (E) Overlay of the average glutamate transients elicited by synaptic stimulation under baseline (black solid),

[A β S26C]₂ application (500 nM, red) and washout conditions (black dashed). **(F)** Overlay of the average glutamate transients elicited by synaptic stimulation under baseline (black solid), TBOA application (10 μ M, blue) and washout conditions (black dashed). **(G)** Box plot of the amplitude of the glutamate transient after the injection of ACSF (left), [A β S26C]₂ (middle) or TBOA (right). N-numbers are indicated next to the boxes. **(H)** Top: representative two-photon images of hippocampal CA1 in vivo under baseline conditions (left), during the application of anti-GLT-1 polyclonal antibody (AB, middle) and after washout (right). The colored dots on the neurons indicate the number of Ca²⁺-transients per minute. Bottom: Ca²⁺- traces of the five neurons circled in the top panel. The shaded area represents the time of AB application. Scale bar: 5 μ m. **(I)** Summary data of the experiment in (H) for n = 6 mice. Error bars show SEM. Kruskal wallis test with Dunn-Sidak post-hoc comparison (G) or Wilcoxon signed rank test (I). **P<0.005, *P<0.05; n.s. not significant.

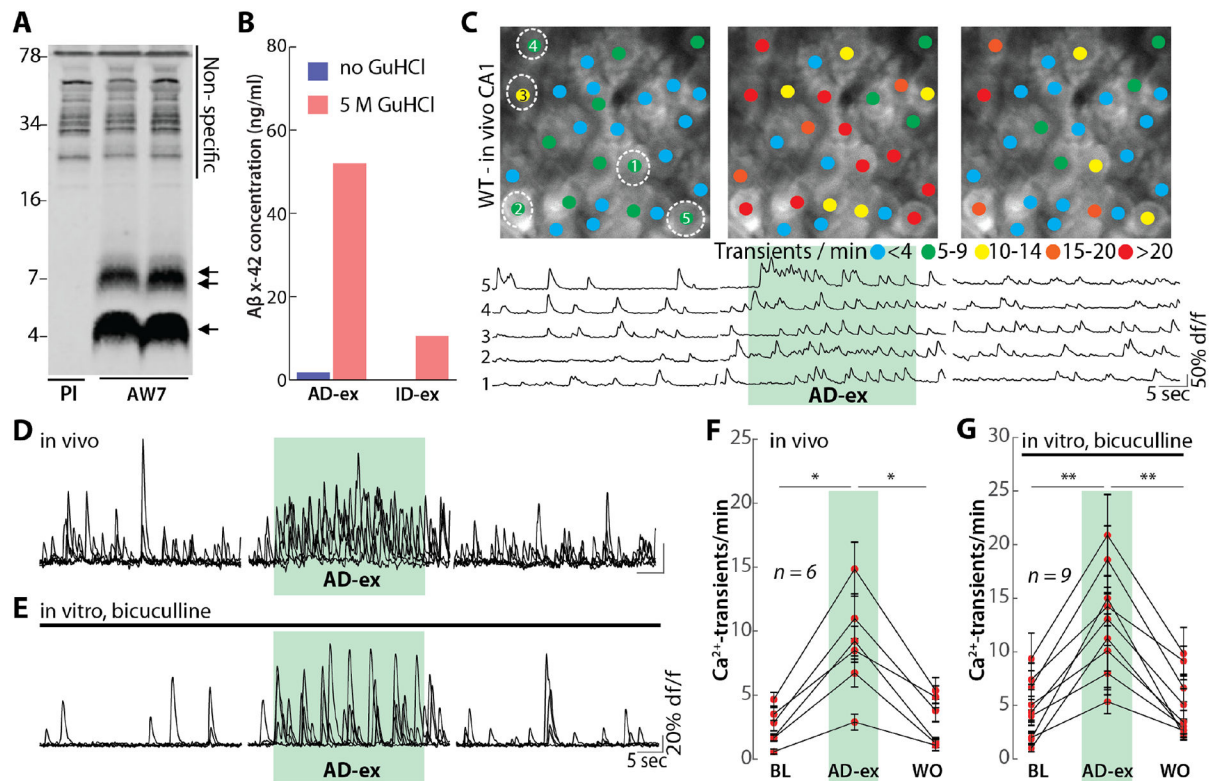


Fig. 4. Aβ derived from human AD patients induces neuronal hyperactivation.

(A) AD brain extracts were immunoprecipitated with anti-Aβ polyclonal antibody AW7 or pre-immune serum (PI) and IP's analyzed by immunoblot using a combination of 2G3 and 21F12. Molecular weight markers are indicated on the left. At least two different Aβ species are in AD brain extract: monomers (single arrow) and SDS-stable Aβ dimers (double arrow). Non-specific bands detected are indicated by a solid black line. (B) Mock immunodepleted (AD-ex) and AW7 immunodepleted (ID-ex) brain extracts were analyzed by an MSD-based Aβx-42 immunoassay. To assess the levels of monomeric and soluble aggregated Aβ, samples were pretreated with or without incubation in 5 M GuHCl. The AD extract contained much higher amounts of aggregates than monomer, and both were effectively removed by AW7 immunodepletion. (C) Top: representative two-photon images of hippocampal CA1 in a wild-type mouse in vivo under baseline conditions (left), during the application of AD-ex (diluted 1:10) and after washout (right). The colored dots on the neurons indicate the number of Ca²⁺-transients per minute. Bottom: Ca²⁺-traces of the five neurons circled in the top panel. The green shaded area represents the time of AD extract application. Scale bar: 5 μm. (D) Overlaid Ca²⁺-traces from 5 representative neurons recorded in vivo under baseline (left), AD-ex application (middle) and washout conditions (right). The green shaded area corresponds to the time of AD extract application. (E) Overlaid Ca²⁺-traces from 5 neurons recorded in vitro in a slice treated with bicuculline under baseline (left), AD-ex application (middle) and washout conditions (right). The green shaded area corresponds to the time of AD-ex application. (F) Summary data for the experiment in (D). Each dot represents the mean number of Ca²⁺-transients per minute for all neurons in one mouse under baseline (BL), AD-ex application and washout (WO) conditions. (G)

Summary data for the experiment in (E). Error bars show SEM. Wilcoxon signed rank test.
** P<0.005, *P<0.05.

Author Manuscript

Author Manuscript

Author Manuscript

Author Manuscript

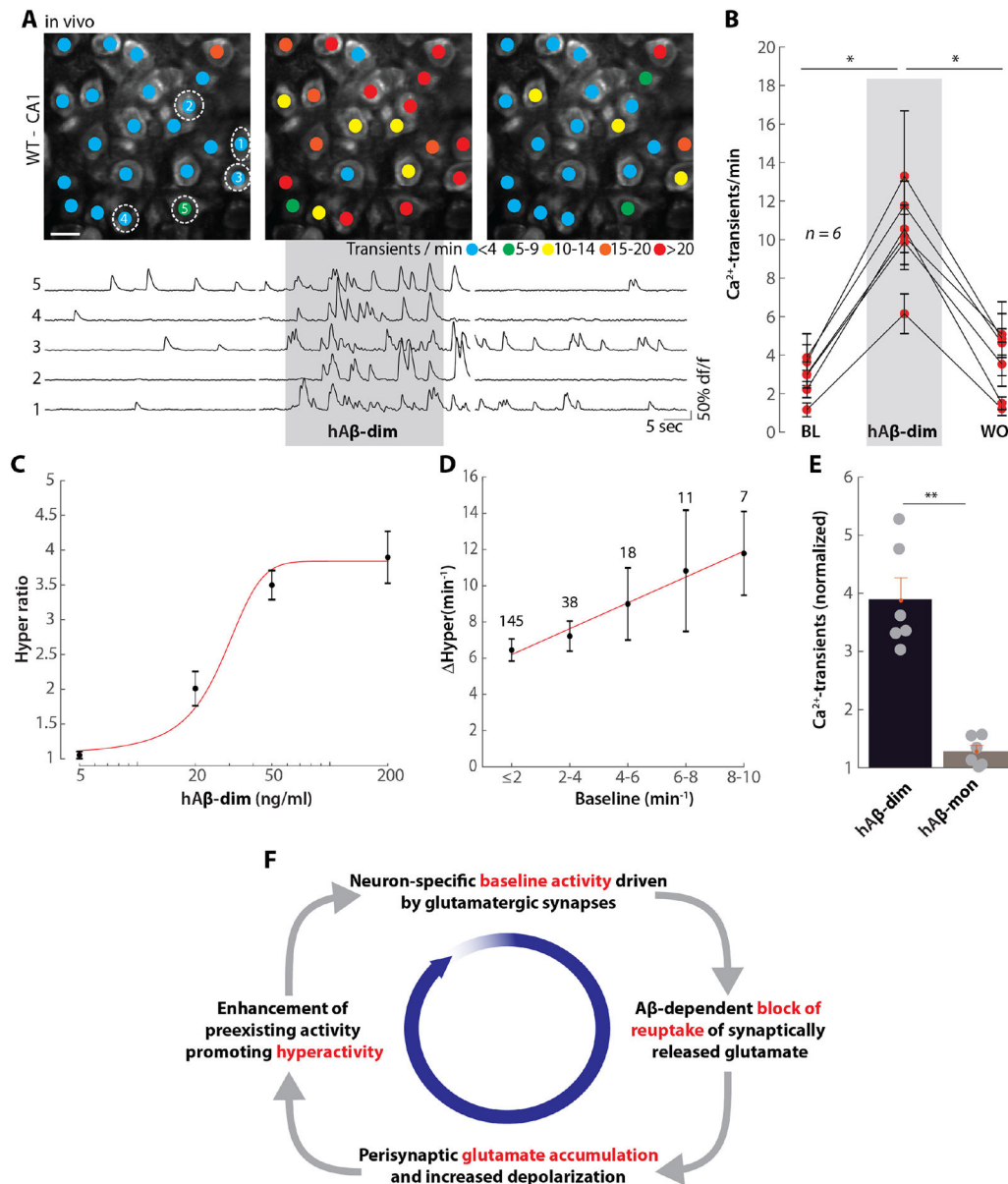


Fig. 5. Role of human Aβ dimers and vicious cycle of hyperactivation.

(A) Top: representative two-photon images of hippocampal CA1 region of a wild-type mouse in vivo under baseline conditions (left), during the application of 200 ng/ml human Aβ dimer (hAβ-dim, middle) and after washout (right). The colored dots on the neurons indicate the number of Ca²⁺-transients per minute. Bottom: Ca²⁺-traces of the five neurons circled in the top panel. The grey shaded area represents the time of hAβ-dim application. Scale bar: 5 μm. (B) Summary data for the experiment in (A). Each dot represents the mean number of Ca²⁺-transients per minute for all neurons in one mouse under baseline (BL), hAβ-dim application and washout (WO) conditions. (C) Dose-dependency curve of the action of hAβ-dim. The activity during hAβ-dim application, normalized to baseline (hyper ratio), for different dilution steps of the human Aβ dimer for 5 ng/ml (n = 5), 20 ng/ml (n = 5), 50 ng/ml (n = 5) and 200 ng/ml (n = 6) are plotted. (D) Plot of baseline activity (BL) vs.

human A β dimer-dependent relative increase in activity in vivo (DHyper) for individual neurons. The numbers of neurons for each bin of BL activity is indicated in the graph. Red line: linear fit. **(E)** Bar graph of the normalized activity during the application of 200ng/ml hA β -dim (left, n = 6) or human A β monomer (hA β -mon, right, n = 6). Each point represents the mean number of Ca²⁺-transients in one mouse during the application, normalized to baseline. Error bars show SEM. Wilcoxon signed rank test (B) or Wilcoxon rank sum test (D), **P<0.005, *P<0.05. **(F)** Scheme of the vicious cycle of A β -dependent neuronal hyperactivation.

Author Manuscript

Author Manuscript

Author Manuscript

Author Manuscript